Malaysian Journal of Science 22: 95-104 (2003)

Molecular dynamics simulations of n-octyl-β-D-glycosides: some structural properties of micelles

Teoh Teow Chong and **Rauzah Hashim**

Department of Chemistry, Faculty of Science, University of Malaya, 50603 Kuala Lumpur, Malaysia

ABSTRACT Micellar structures of n-octyl-β-D-maltopyranoside (OM) and n-octyl-β-D-glucopyranoside (OG) were investigated using molecular dynamics simulation. The gyration radii of OM and OG micelles were compared. In order to investigate the effect of head group, the micellar structure of n-octyl-β-D-galactopyranoside (Ogal) was also studied. It was found that OG formed bigger micelles with gyration radii ranging from 7.18 to 11.62Å. OM formed a small micelle with gyration radius of 8.21Å and Ogal formed micelles with gyration radii ranging from 8.66 to 11.07Å.

ABSTRAK Struktur misel n-octyl-β-D-maltopyranoside (OM) dan n-octyl-β-D-glucopyranoside (OG) telah dikaji dengan simulasi dinamik molekul. Jejari gyrasi misel OM dan OG dibandingkan. Untuk mengkaji kesan kumpulan kepala, struktur misel n-octyl-β-D-galactopyranoside (Ogal) juga telah dikaji. Didapati bahawa OG membentuk misel yang lebih besar dengan jejari gyrasi berukuran 7.18 ke 11.62Å. OM membentuk misel yang kecil dengan jejari gyrasi berukuran 8.21Å manakala Ogal membentuk misel dengan jejari gyrasi berukuran 8.66 ke 11.07Å.

(Micelle, molecular dynamics, Amber forcefield, gyration radius, reversed micelle)

INTRODUCTION

Alkyl glucosides constitute a new and interesting class of surfactant and these are available commercially (for example ANAGRADE® (0311) and SOL-GRADE® (0311S)[1]). Octyl glucoside is an example of the extensive use of glycolipids as nonionic detergent consist of an octane attached to a sugar Figure 1. As expected for a nonionic surfactant, solution of alkyl glucosides are insensitive toward the addition of salt [2, 3, 4]. There are several indications that it is the complex isomerism of the carbohydrate head group that determine the physico-chemical properties of alkyl glucosides [5, 6, 7, 8]. They have been used to stabilize, reconstitute, purify and crystallize membrane proteins and membrane- associated protein complexes without denaturation. Aqueous solutions of the glucosides from octyl through dodecyl foam on shaking but dodecylglucoside is only slightly soluble in cold water [9]. Thus, octyl glucoside was used for the purification of the intact serine receptor to study the ligand site of a bacterial chemotaxis membrane receptor [10] and it has been of interest as an emulsifier, a cleaning agent and a drug carrier due in part to its nontoxic and biodegradable nature [11]. This biodegradable nature is due to the formation and breakdown of alkyl glucosides which are enzymatically controlled by different glucosidases [12, 13]. The discussion above illustrates the commercial importance of the material which requires the support of fundamental studies.

Mono alkyl glycosides have been extensively studied experimentally as reported in the literature. For these compounds, generally small modifications in chemical structure can lead to a large change in the phase behavior (see for example a recent review by Vill and Hashim [14]), in particular, on the melting point, the clearing point, the solubility in water, and the extent of the lamellar and curved phases [15]. The n-alkyl-β-D-glycopyranosides (AGs) have been shown to exhibit thermotropically liquid crystal phases by X-ray diffraction and calorimetric investigations [16, 17, 18]. The AGs possess a single liquid crystal mesophase which was suggested to be of a smectic nature. Powder diffraction X-ray studies of this phase produced a single diffuse ring of scattering similar to those obtained for smectic A phases [19, 20].

In the lyotropic system, the lamellar phase of n-octyl-β-D-galactopyranoside (Ogal) has a bilayer spacing of 25.1Å, smaller than the value of 29.3 Å for n-octyl-β-D-glucopyranoside (OG). However, the d-spacing of the Ogal smectic A phase, 25.8 Å, is similar to the corresponding value for OG. The biggest difference between Ogal and OG is the much greater temperature stability of the crystalline lamellar phase. The Ogal solid melted at 96°C and the smectic phase was stable up to 127°C, and the OG solid melted at 69°C and the smectic phase was stable up to 116°C, respectively [15]. Unfortunately, data for OM is not available now and further studies are underway to investigate it in some detail in the future either experimentally or *in silico*.

Extensive computational studies have been reported in the literatures on biological membranes ranging from simple Monte Carlo lattice models [21] to sophisticated molecular dynamics simulations [22]. However only a few can be found for glycolipids despite their importance in biological systems such as lipid bilayers, miscelles and liposomes and in other areas of technology, especially surfactant systems, mainly because suitable force fields for carbohydrates were not so widely available especially on commercial software. It is only recently that such force fields for carbohydrates were incorporated for software like CHARMM [24, 25]. Some of the early molecular dynamics simulation on glycolipids were carried out to investigate the micellar system [11, 23] for octyl glucosides.

Experimentally, alkyl glucosides with β-linkage are more soluble in water, have higher cmc values (17 mM for OG and a lower 5.8 mM for Ogal)[26], lower Krafft points, and form smaller aggregates at dilute concentration than the alkyl glucosides with α-linkage [27]. The binary phase diagram for OG has been determined independently by Sakya et al. [28] and Nielsson et al. [27] where a penetration experiment was performed for a whole concentration range of the binary phase diagram from neat water to neat OG simultaneously.
They showed that below 20°C, a micellar solution, a hexagonal liquid crystalline phase, an isotropic region (a cubic phase) and finally a lamellar phase liquid crystalline phase were formed. It is not possible to observe any two-phase regions between the phases. Above 22°C, the hexagonal phase has melted and the micellar solution is in equilibrium with the cubic phase. At still higher temperatures, there is only a micellar solution in equilibrium with the lamellar phase (75wt% OG) [27,28].

From the binary phase diagram for OG/water, below 20°C, the region examined (0- 94.8wt% OG) there are five different phases present. From 60 to 70wt% OG, there is an anisotropic phase of hexagonal texture. Above 22°C the hexagonal phase melts into an isotropic solution. In the region from 70 to 80wt% OG, there is a very stiff non-fluid isotropic region. This region has been determined to be a cubic liquid crystalline phase. The cubic phase melts at a temperature slightly above 50°C and forms a less viscous (fluid) isotropic solution. When the concentration is increased to more than 80wt% OG, a lamellar phase is formed. At high concentrations (above 93wt%), the lamellar phase is in equilibrium with hydrated crystals.

The extensive isotropic region from neat water to ca. 60wt% OG suggests the surfactant aggregates remain relatively small and do not grow into extended rods. Moreover the aggregate-aggregate interaction is relatively short-ranged hence no ordering of the aggregates takes place. One possible explanation for the aggregates to remain relatively small was that the area available for the glucose molecules at the hydrophobic/ hydrophilic interface is limited, and it is unfavorable to vary that area by increasing the aggregate size [27].

The short-ranged aggregate-aggregate interaction of alkyl glucosides has been established by direct surface force measurements [29]. This fact implies that two aggregates can come in close proximity to each other, and as a consequence, the system may be disordered up to high volume fractions of aggregates.

Another interesting feature of the phase diagram is the fact that the hexagonal phase melts at a relatively low temperature (around 22 °C), while the cubic phase melts at a comparatively higher temperature. It has been suggested [30] that this implies the micellar structure (at least close to the phase boundary with the cubic phase) can be described as a melted cubic phase. Since the cubic phase is bicontinuous, this implies that the micellar microstructure is also bicontinuous, in that the micelles form a connected network.

As a function of micelle size, effective micellar radius, R and radius of gyration, R_G were calculated [23]. Assuming the micelles formed are spherical and the spheres are hollow,

$$R = \sqrt[3]{\frac{3V}{4\pi}} \quad \text{and} \quad R_G = \sqrt{\frac{2}{3}R^2}$$

These equations define R_G^2 as the ratio of volume per circumference.

A similar equation used in computing the radius of gyration is given by Bogusz et al. [23] namely $R_G = \sqrt{\frac{3}{5}R^2}$, which most probably considered the spheres as solid spheres (for solid spheres, $R_G = \sqrt{\frac{2}{5}R^2}$) defined by the author for lyotropic systems.

VanAken et al. and Lorber et al. reported R_G= 16.8Å for 27mer, which is slightly larger than the experimental result of 15 Å for purported 27mers [31, 32].

Bogusz et al. [23] also reported the linear relationship between the radius of gyration (R_G) and the number of lipids (N) for OG micelles. The linear relationship for Ogal and OM is still not known. Besides that, he reported the formation of micelles consist of 5, 10, 20, 27, 34, 50 and 75 lipids. In his simulation, 500 lipids were used and he rotated the lipid until the tail was pointing inward to form a roughly micelle structure.

Besides obtaining the critical micelles concentrations or cmc, the purpose of generating micelles is also to obtain more complicated shapes such as liposomes. If drugs or bioactive compounds are engulfed by the micelles or liposomes generated, then drug carrier mechanism through the plasma membrane can be studied. In addition, using the liposomes, further studies of the interactions among cells, drugs and antigens such as bacteria and viruses would be possible.

The purpose of the present work is to investigate the micellar structure of n-octyl-β-D-maltopyranoside (OM) and n-octyl-β-D-glucopyranoside (OG) using molecular dynamics simulation *in vacuo* and to compare with experimental results obtained by Niemeyer et al. [33, 34]. The gyration radii of OM and OG micelles were compared. In order to investigate the effect of the head group, the micellar structure of n-octyl-β-D-galactopyranoside (Ogal) was also studied. The only difference between Ogal and OG is that the C4-linked hydroxyl group in Ogal is axial while that in OG is equatorial. The chemical structures of OG, Ogal and OM are shown in **Figure 2(a)**, **(b)** and **(c)** respectively.

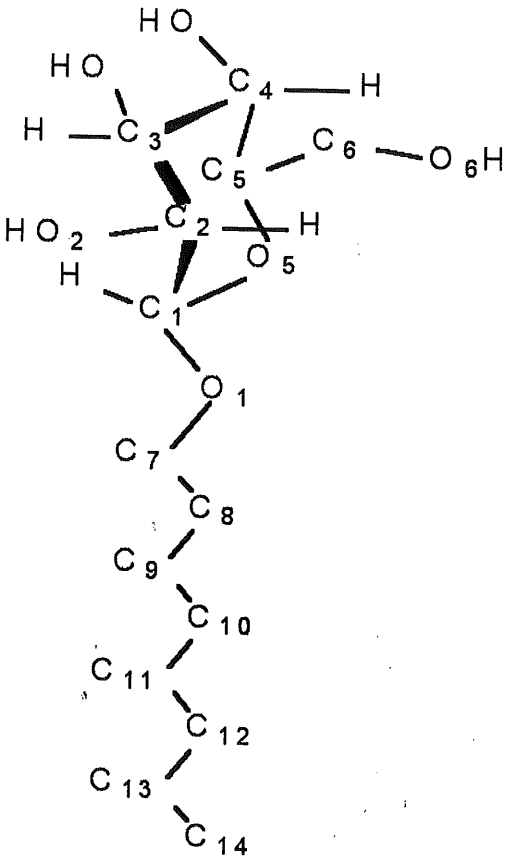

Figure 1. β-octyl glucoside with heavy atom numbering scheme

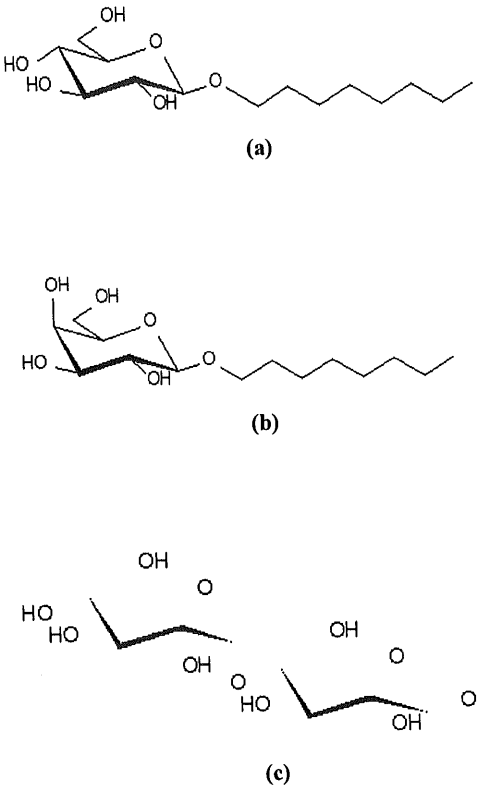

Figures 2. The chemical structures of β-octyl glucoside, β-octyl galactoside and β-octyl maltoside, respectively.

MATERIALS AND METHODS

Simulations were carried out with the HyperChem simulation package version 6.01, 2000 for Windows. The force field parameters used were those from Amber specifically developed for saccharides [35]. Parameters for linking the sugar head to the octane tail were based on Amber parameters (Table 1). The Lennard-Jonnes interactions were truncated between 10 and 14Å with a smooth switching of the potential. A default electrostatic interaction scale factor of 0.833 and 0.5 of van de Waals interactions scale factor were used.

OM, OG and Ogal were modeled using the Amber forcefield and geometrically minimized with steepest decent algorithm (SD) with RMS gradient of 0.1 kcal/(Åmol) *in vacuo*.

To generate a series of starting configurations, we modified the method used by Bogusz et al. [23] in which 100 n-octyl-β-D-glycosides were arranged in lamellar form (because at high concentrations, OG forms lamellar phase which is in equilibrium with micelles) [15] and were geometrically minimized with a steepest decent algorithm (SD) with RMS gradient of 0.1 kcal/(Åmol) *in vacuo*. After minimization, molecular dynamics (MD) was applied to the system at 298K for 20ps. A step size of 0.001 ps was used and data was recorded for every time step. This enables a continuous analysis of the evolution of kinetic energy, potential energy, total energy and temperature. A series of random micelles obtained were named according to the number of lipid monomers present in one micelle (for example, 10mer, 12mer, etc).

Computer simulation using a realistic model such as the one attempted here is a challenging task in terms of computational power. Even for other non-glycolipid bilayer systems (such as DPPC), computer simulation studies were confined to small sample sizes. For example a simulation of a 72 lipid/water system running for 170 ps in 2000 would have required six months of computational time! (see Pastor et al. [36]). The simulation of a system of 100 lipids/water) for 10-100 ns has become feasible only recently [37]. To reduce the computational time, sometimes it is necessary to use "cheaper" numerical algorithms; for example energy minimization could be performed *in vacuo* using a quasi-Newton-Raphson method while a steepest descent algorithm was applied in solvated system [34]. Therefore our preliminary simulation work for glycolipids, although it is modest, is aimed to prove initial concepts rather than to reproduce accurate results. Further studies are necessary including conducting the simulation in water.

Error Estimation

The χ^2 (chi-squared) test was performed on the data obtained. This test allows us to compare our observed results with the expected results, which in this case are those of [23], and decide whether or not there is a significant difference between them.

$\chi^2 = \Sigma\left[\frac{(O-E)^2}{E}\right]$, where Σ denotes summation and O and E are the observed and the expected values, respectively.

Table 1. Calculated bond lengths for OG, OM and Ogal. The bond lengths for OG in Italics are those from Bogusz et al. [23].

	OG	OM	Ogal
Bond	**Minimized bond length (Å)**		
C7-O1	1.4215 (*1.4450*)	1.4264	1.4218
C1-O1	1.4220 (*1.4066*)	1.4246	1.4289
Angle	**Minimized bond angle (°)**		
O1-C7-C8	110.918 (*105.000*)	110.934	108.597
O1-C7-H7	110.008 (*107.240*)	110.393	109.779
O1-C1-C2	107.763 (*107.602*)	111.587	109.400
O5-C1-O1	109.592 (*115.732*)	107.584	111.052
H1-C1-O1	109.357 (*109.385*)	109.430	106.538
C1-O1-C7	112.764 (*107.500*)	112.852	114.552
Dihedral	**Minimized bond angle (°)**		
O1-C1-O5-C5	177.720	172.292	-74.931 (285)
C3-C2-C1-O1	175.994	175.206	81.701 (278.29)
O1-C1-C2-H2	56.407	54.727	-37.366 (322.6)
O1-C1-C2-O2	-62.626	-65.106	-153.727
C7-O1-C1-O5	-74.676	-70.938	-70.357
C2-C1-O1-C7	166.646	170.766	163.143
C8-C7-O1-C1	164.488	154.384	-170.186 (189.814)

RESULTS AND DISCUSSIONS

Table 1 shows the potential parameters for OG, OM and Ogal for regions linking sugar head and octane tail after minimization.

The OG results for bond lengths and angles were compared with a previous calculation [23] given in italics (Table 1) using the CHARMM [37] forcefield [24,25] and the Adopted Basis Newton-Raphson (ABNR) algorithm for the minimization. However, a statistical comparison χ^2 (chi-squared) demonstrated an error of less than 1% between the two set of results. The χ^2 for bond length is 0.00055 (critical value = 1.32) and the χ^2 for bond angle is 1.14 (critical value = 6.63) for a probability of 0.25 for both cases. Therefore, we can conclude that our calculation for the structural properties of these glycolipids is reliable qualitatively and comparable with those of Bogusz et al. [23].

Comparing our calculated results for the various glycolipids (OG, OM and Ogal), it was found that the bond lengths of these are similar to within less than 1%. However the variations in bond angles between them are quite significant as to be expected. First the glycosidic bonds linking to the octyl tail (O1-C7-C8 and O1-C7-H7) for OM and OG and Ogal are similar within less than 1% error. But for the glycosidic bonds linking to the sugar groups the variations between them are as high as 3-4% which further shows that constituents and conformations of the head groups affects the overall behavior of these glycolipids.

While the dihedral angles of OG and OM were found to be quite similar to within less than 5%, however those for Ogal were, however, found to be significantly different from the former two. The stereochemistry of Ogal at the fourth carbon (C4) position play a significant role in these variations of the dihedral angles and this is further reflected in the difference of bulk properties of OG and Ogal as reported in [15].

The physical properties of micelles generated are shown in (Table 2) for 100 lipid molecules in each of OG, OM and Ogal. OG formed four micelles each contains 18mer, 10mer, 5mer and 4mer; Ogal formed four micelles containing 16mer, 12mer, 10mer and 7mer while OM formed only one micelle of 4mer. These showed that the micellar aggregation number of OM is smaller than that of OG and these results were in agreement to those obtained by Niemeyer et al. [33]. In addition, the gyration radii of OM (8.21 Å) are smaller than that of OG (11.62 Å) and Ogal (11.07 Å). However Niemeyer et al. [33] reported the gyration radii of OG and OM dissolved in D_2O determined using a Small Angle Neutron Scattering (SANS) experiment were 27.7 Å and 14.4 Å. In a similar experiment but under slightly different conditions, they found the radius of gyrations for OG and Ogal were similar

namely 29.8 Å and 25.4 Å respectively. Although our calculated values did not agree quantitatively with those obtained by Niemeyer et al. [33] as to be expected, qualitatively the two sets of results showed a similar trend as far as the effect of the size of the headgroup to the gyration radii is concerned.

These results indicate that increasing the size of the sugar head group decreases the stability of the spherical micelles. However OM also gave elongated micelles (20mer, 32mer and 44mer) not observed in OG and Ogal. Hence it can be concluded that the increased size of head group of OM supports the formation of non-spherical micelles.

Figure 3 below shows the relationship between the radius of gyration (R_G) and the number of lipids $(N)^{1/3}$ for OG micelles. From the results, it was found that the radius of gyration, R_G versus the number of lipid, (N) to the 1/3 power for both OG(continuous line) and Ogal (broken line) show a linear relationship and these results are similar to that obtained by Bogusz et al. [23], which again indicates a satisfactory qualitative agreement.

Table 2. The physical properties of aggregate structures for OG, Ogal and OM 100 n-octyl-β-D-glycosides were arranged in lamellar form and geometrically minimized with steepest decent algorithm (SD) with RMS gradient of 0.1 kcal/(Åmol) *in vacuo*. After minimization, molecular dynamics (MD) was applied to the system at 298K. A step size of 0.001 ps was used and data was recorded for every time step.

Octyl glycosides	Partial harges, (e)	Radius[1] R (Å)	Gyration Radius[21], R_G (Å)	$N^{1/3}$	Volume, (Å^3)	Mass (amu)
OG						
18mer	0	14.23	11.62	2.62	12061.13	5262.71
10mer	0	11.94	9.75	2.15	7123.42	2923.73
5mer	0	9.55	7.80	1.70	3647.53	1461.86
4mer	0	8.79	7.18	1.59	2843.97	1169.49
Ogal						
16mer	0	13.56	11.07	2.52	10453.39	4677.96
12mer	0	12.48	10.19	2.30	8144.67	3508.47
10mer	0	11.73	9.58	2.15	6767.68	2923.73
7mer	0	10.61	8.66	1.91	5001.71	2046.61
OM						
4mer	0	10.05	8.21	1.59	4251.56	1818.06

[1]Radius, $R = \sqrt[3]{\frac{3V}{4\pi}}$

[2]Radius of Gyration, $R_G = \sqrt[2]{\frac{2R^2}{3}}$

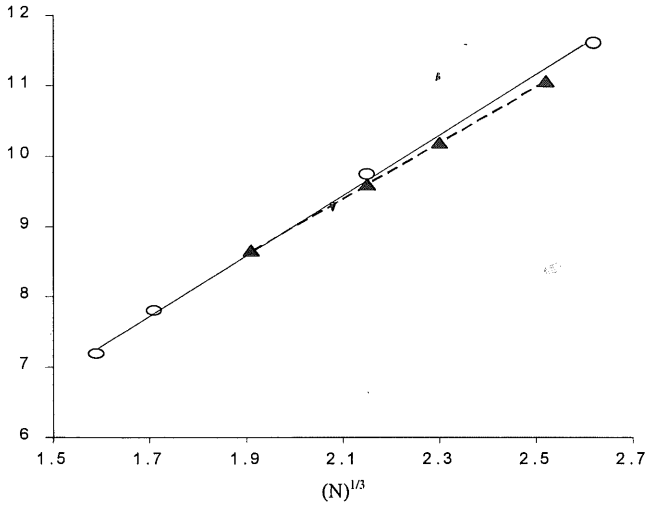

Figure 3. Radius of gyration, R_G vs number of lipids, (N) to the 1/3 power for OG(open circle) and Ogal (filled triagle). Given also the lines of regression for OG(continuous) and OM (dotted).

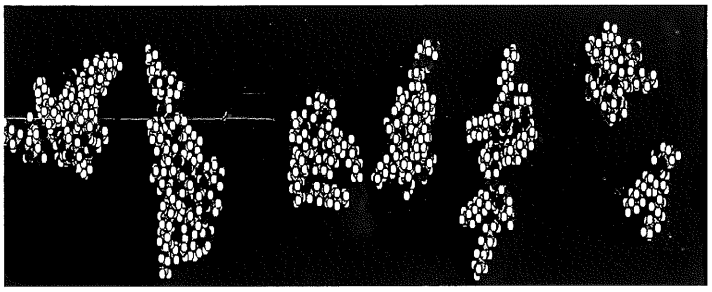

(a) **OG**

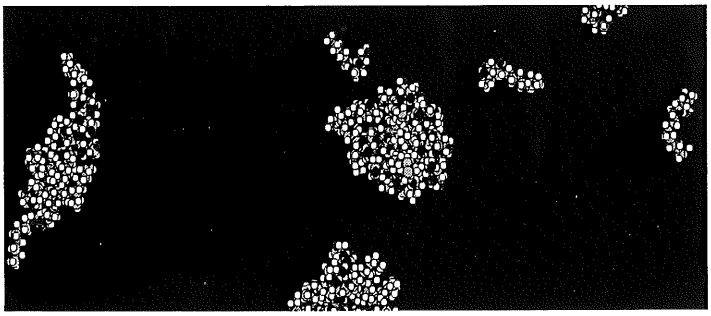

(b) **Ogal**

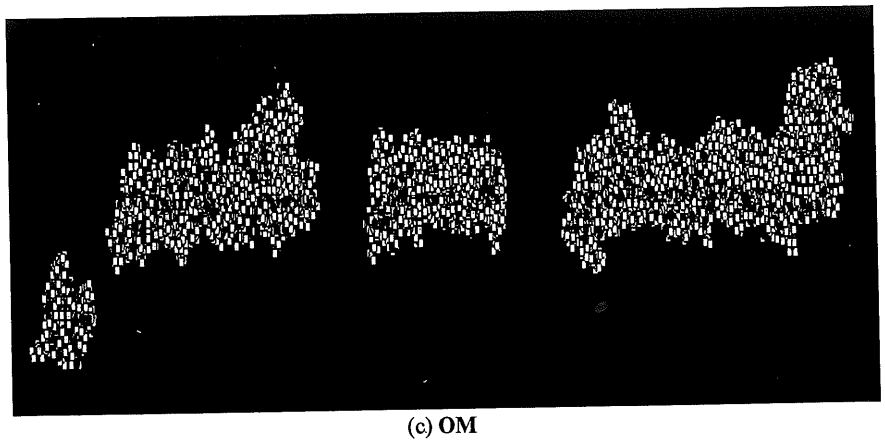

(c) **OM**

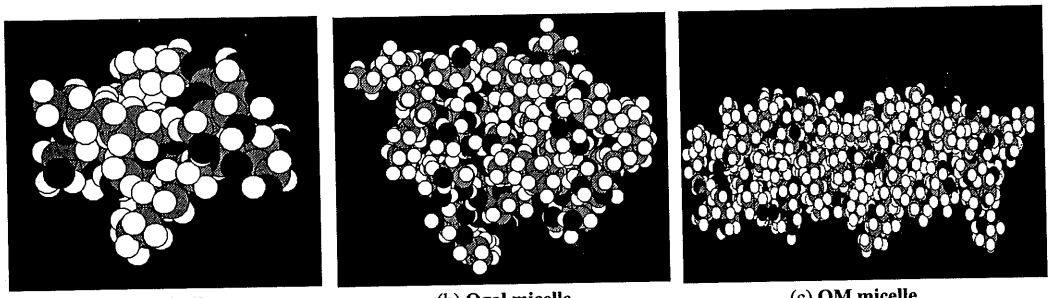

(a) **OG micelle** (b) **Ogal micelle** (c) **OM micelle**

Figures 5. OG and Ogal micelles

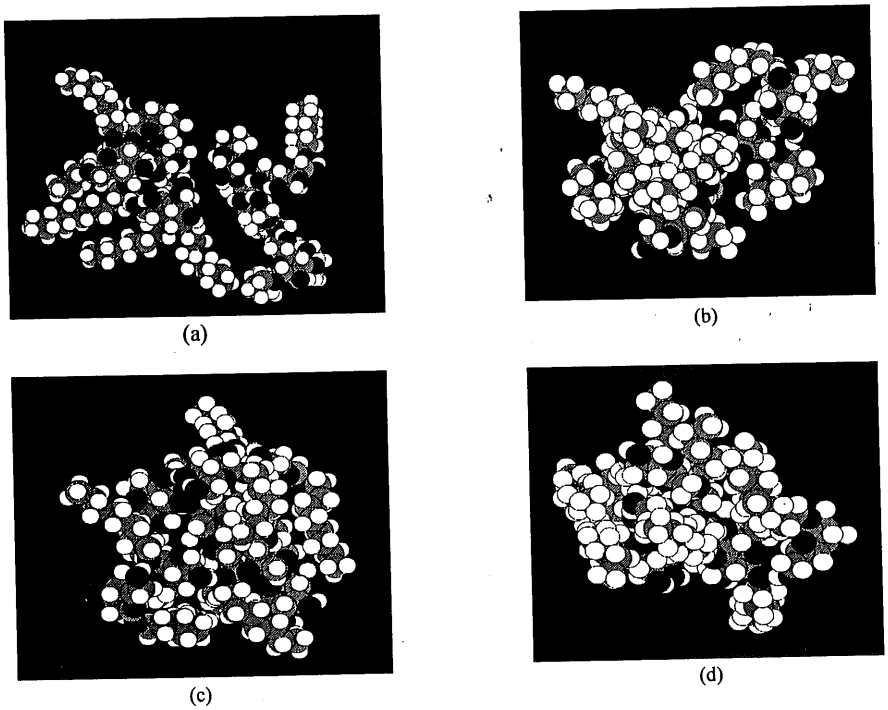

(a) (b) (c) (d)

Figures 6. The evolution of 10mer OG micelle during the course of simulation.

Figures 4 (a), (b) and (c) show the structures of final configurations for OG, Ogal and OM micelles, respectively. Figures 5 (a), (b) and (c) show the single micelles for OG, Ogal and OM, respectively. It was observed that for OG and Ogal, the results obtained were similar in that the lipid bilayer structures formed micelles. On the other hand, OM only formed one micelle and the remaining lipids formed non-spherical shape micelles (20mer, 32mer and 44mer).

Figures 6 (a) to (d) show that the OG micelles generated are reversed micelles as the tails are pointing outward and the glucose heads are pointing inward. As expected for a simulation in vacuum, Ogal and OM gave similar micellar arrangements.

CONCLUSIONS

We have presented initial studies on three octyl glycosides (glucose, galactose and maltose) using molecular dynamics calculations. Our simple calculations for octyl glucoside (OG) agreed qualitatively with the more extensive calculation performed by Bogusz et al. [23]. To our knowledge there have been no previous calculations for galactose and maltose analogues for comparison. It was found that OG formed bigger micelles with a gyration radius of 11.62Å with 18 monomers. OM formed micelle with gyration radius of 8.21 Å with 4 monomers and Ogal formed micelles with a gyration radius of 11.07Å with 16 monomers. The micelles generated are reversed micelles with the tails pointing outward and the glucose heads are pointing inward.

Acknowlegments We are grateful to MOSTE for a research grant given to support this study.

REFERENCES

1. Anatrace Catalog 2002/2003, 3rd Edition July, 2002 at
2. http://www.anatrace.com/Literature/Anatrace%20Catalog%20%203rd%20Edition.pdf
3. Focher B., Savelli, G., Torri, G., Vecchio, G., Mc Kenzie, D.C., Nicoli, D.F. and Button, C.A. (1989). Chem. Phys. Lett., **158**: 491.
4. Fukuda, K., Soderman, O., Lindman, B. and Shinoda, K. (1993). Langmuir, **9**: 2921.
5. Kameyama, K., and Takagi, T. (1990). J. Colloid Int. Sci., **137**: 1.
6. Balzer, D. (1991). Tenside Surf. Det., **28**: 419.
7. Hughes, F.A. and Lew, B.W. (1970). J. Am. Oil Chem. Soc., **47**: 162.
8. Parker, W.O., and Genova, C. (1993). J. Carignano, G. Colloid Surf. A, **72**: 275.
9. Straathof, A.J.J., van Bekkum, H. and Kieboom, A.P.G. (1988). Starch, **40**: 438.
10. Noller, C.R. and Rockwell, W.C. (1938). J. Am. Chem. Soc. **60**: 2076.
11. Wang, J., Balazs, Y.S. and Thompson, L.K. (1997). Biochemistry, **36**: 169- 1703.
12. Bogusz, S., Venable, R.M. and Pastor, R.W. (2001). J. Phys. Chem. B, **105**: 8312-8321.
13. Stryer, L. (1988). Biochemistry, 3rd ed., W.H. Freeman and Company, New York.
14. Pigman, W.W. and Ritchmeyer, N.K. (1942). J. Am. Chem. Soc. **64**: 369.
15. Vill, V. and Hashim, R. (2002). Current Opinion in Colloid and Interface Science, **7**: 5-6, 395-409.
16. Sakya, P., Seddon, J.M. and Vill, V. (1997). Liquid Crystals, **23**(3), 409-424.
17. Carter, D.C., Ruble, J.R. and Jeffrey, G.A. (1982). Carbohydr. Res., **102**:59.
18. Jeffrey, G.A. and Bhattacharjee, S. (1983). Carbohydr. Res., **115**: 53.
19. Dorset, D.L. and Rosenbusch, J.P. (1981). Chem. Phys. Lipids, **29**: 299.
20. Leadbetter, A.J., Durrant, J.L.A. and Rugman, M. (1977). Mol. Cryst. Liq. Cryst. Lett., **39**: 231.
21. Leadbetter, A. J., Frost, J.C., Gaughan, J.P. Gray, G.W. and Mosely, A. (1979). J. Phys (Paris), **40**: 375.
22. Goodby, J.W. (1984). Mol. Cryst. Liq. Cryst. **110**: 205-219.
23. Xing L. and Mattice, W.L. (1998). Langmuir, **14**: 4074.
24. Pastor, R.J., and Venable, R.M. (1993). Computer Simulations of Biomolecular systems; van Gunsteren, W.F., Weiner, P.K. and Wilkinson, A.J.,. Eds., Escom: Leiden, **2**: 443.
25. Bogusz, S., Venable, R.M. and Pastor, R.W. (2000). J.Phys.Chem.B, **104**: 5462-5470.
26. Ha, S.N., Giammona, A., Field, M. and Brady, J.W. (1988). Carbohydrate Res. **180**: 207.
27. MacKerell, A.D., Bashford, D., Bellott, M., Dunbrack, R.L., Evanseck, J.D., Field, M.J., Fischer, S., Gao, J., Guo, H., Ha, S., Joseph-McCarthy, D., Kuchnir, L., Kuczera, K.,

Lau, F.T.K., Mattos, C., Michnick, S., Ngo, T., Nguyen, D.T., Prodhom, B., Reither, W.E., Roux, B., Schlenkrich, M., Smith, J.C., Stote, R., Straub, J., Watanabe, M., Wiorkiewicz-Kuczera, J., Yin, D. and Karplus, M. (1998). J. Phys.Chem. B. **102**: 3586.

28. Vill, V. Liquid Crystals Database Version 4.2. Copyright © 2002 at http:// liqcryst.chemie.uni-hamburg.de
29. Nielson, F., Soederman, O. and Johansson, I. (1998). Langmuir **14**: 4050-4058,
30. Sakya, P., Seddon, J.M. and Templer, R.H. (1994). J.Phys.II France, **4**: 1311.
31. Waltermo, A., Manev, E., Pugh, R. and Claesson, P. (1994). J. Disp. Sci. Tech. **15**: 273.
32. Monduzzi, M., Olsson, U. and Soderman, O. (1993). Langmuir, **9**: 2914.
33. VanAken, T., Foxall-VanAken, S., Castleman, S., Ferguson-Miller, S. (1986). Meth. Enzymol., **125**: 27.
34. Lorber, B. Bishop, J.B. and DeLucas. L. (1990). J.Biochim. Biophys. Acta, 1023, 254.
35. Niemeyer, B., He, L.-Z., Haramus, V., Helmholz, H. and Willumeit, R., (2000). GKSS SANS-1 Experimental Report.
36. Lizhong He, Garamus, V.M., Funari, S.S., Malfois, M., Willumeit, R. and Niemeyer, B., (2002). J. Phys. Chem. B. **106**: 7596-7604.
37. Homans, S.W. (1990). Biochemistry **29**: 9110-9118.
38. Pastor, R.W. and Venable, R.M., (2002). Account of Chemical Research, **35**: 438-446.
39. Brooks, B.R., Bruccoleri, R.E., Olafson, B.D., States, D.J., Swaminathan, S. and Karplus, M., (1983). J. Comput. Chem. **4**: 187.